International Journal of Environmental Science and Technology (2021) 18:2831–2846
https://doi.org/10.1007/s13762-020-03031-1

ORIGINAL PAPER

Effect of cobalt complexes on cobalt oxide particles for the activation of peroxymonosulphate in textile wastewater treatment

W. Heuvel[1] · B. Sone[1] · V. Fester[1]

Received: 25 February 2020 / Revised: 16 October 2020 / Accepted: 16 November 2020 / Published online: 2 January 2021

Abstract

This study provides a comparison of the chloride and nitrate anions, water and alcohol solutions in the formation of cobalt complexes, and their effect on the cobalt hydroxide polymorph formed and the subsequent impact on the catalytic performance of the resulting cobalt oxide. The formation of α- and β-cobalt hydroxide polymorphs as precursors to Co_3O_4 nanoparticles depended on the cobalt complex formed. In water only, the role of the anion on the phase of hydroxide polymorph is negligible. Annealed Co_3O_4 nanoparticles derived from the solvothermal synthesis of β-cobalt hydroxide using cobalt chloride hexahydrate dissolved in 100% alcohol performed better in sulphate radical-advanced oxidation of methylene blue than annealed Co_3O_4 particles derived from the hydro/solvothermal synthesis of α-cobalt hydroxide using cobalt nitrate hexahydrate dissolved in 50% alcohol. However, when impurities exist in samples produced from nitrate precursor salts, the performance of the α-cobalt hydroxide-derived Co_3O_4 noticeably improves. This study shows, for the first time, the relationship between the cobalt hydroxide polymorph and the catalytic performance of the resulting Co_3O_4.

Keywords Co_3O_4 · Cobalt hydroxide · Cobalt/pms process · Polymorph · Solvo/hydrothermal synthesis

Introduction

Amongst various transition metals and their oxides, cobalt oxide (Co_3O_4) has been studied for its widespread uses in sensors, energy storage devices (magnetic, electric, optoelectric), as well as its rapid catalytic activity (Athawale et al. 2010; Gamonchuang et al. 2016; Huang et al. 2014; Yang et al. 2004). It also shows thermodynamic stability (Warang et al. 2013) and has been considered the best activator of peroxymonosulphate (PMS)-derived sulphate radicals employed in catalytic degradation of industrial effluent (Rivas et al. 2009; Anipsitakis and Dionysiou 2003).

It may be synthesised through various methods using a cobalt salt along with a source of hydroxyl ions such as ammonium hydroxide (Huang et al. 2014). The following reactions take place during the preparation and hydrothermal synthesis of cobalt oxide:

$$NH_4OH \rightarrow NH_4^+ + OH^-$$

When using cobalt chloride aqueous solution:

$$CoCl_2 \rightarrow Co^{2+} + 2Cl^-$$

When using cobalt nitrate aqueous solution:

$$Co\left(NO_3\right)_2 \rightarrow Co^{2+} + 2\left(NO_3\right)^-$$

Resulting in:

$$Co^{2+} + 2OH^- \rightarrow Co(OH)_2$$

Which when annealed in air yields:

$$6Co(OH)_2 + O_2 \rightarrow 2Co_3O_4 + 6H_2O$$

The use of alcohols in nanoparticle synthesis can provide a means of morphology control, as the properties of alcohols change with increasing alkyl chain lengths (Chowdhury

Communicated by Binbin Huang.

Electronic supplementary material The online version of this article (https://doi.org/10.1007/s13762-020-03031-1) contains supplementary material, which is available to authorised users.

✉ V. Fester
festerv@cput.ac.za

[1] Flow Process and Rheology Centre, Faculty of Engineering & the Built Environment, Cape Peninsula University of Technology, Cape Town, South Africa

et al. 2015; Athawale et al. 2010; Gamonchuang et al. 2016; He et al. 2004). Due to this change in properties, alcohols provide noticeable differences in systems using alcohol/water mixtures. In an aqueous or alcohol medium, metals from the 3d group form complexes. These complexes may be identified by noticeable optical changes, such as those of Co^{2+} cations in aqueous and alcoholic solution which are evident at room temperature when using $CoCl_2{\cdot}6H_2O$ (Petkova and Nedkov 2013). These experiments showed that the colour of the aqueous solution was pink, whereas the alcohol solution was blue, when dissolving $CoCl_2{\cdot}6H_2O$. The cobalt complexes formed were therefore octahedral and tetrahedral, respectively. It was concluded that the reason for a difference in colour lies in the spectral positioning of the 3d electrons, leading to a difference in optical properties (Petkova and Nedkov 2013). The role of the anion on the cobalt complex was not reported. Cobalt hydroxide can readily be obtained when an alkali metal hydroxide is added to the solution.

Cobalt hydroxide, a common precursor to Co_3O_4, exists as one of two polymorphs–alpha cobalt hydroxide-α-$Co(OH)_2$ and beta cobalt hydroxide-β-$Co(OH)_2$, most obviously recognised by their colours green and pink, respectively (Al-Ghoul et al. 2010). The α-$Co(OH)_2$ has a hydrotalcite-like structure, with positively charged layers separated by anions occupying the interlayer spacing, thereby ensuring neutrality. Such solids are often termed Layered Double Hydroxides (LDH) or anionic clays, as they store anions along with water molecules between their positively charged layers (Cheng et al. 2014; Mishra et al. 2018). Solids with this type of structure have been found to be useful as anion exchangers, catalysts, adsorbents, photo-functional materials and active electrode materials (Cheng et al. 2014; Meng et al. 2017). Also, α-$Co(OH)_2$ has a much larger interlayer spacing (> 0.7 nm) versus β-$Co(OH)_2$ (0.46 nm), due to water molecules and charge balancing interstitial anions (Cl^-, NO_3^-, CO_3^{2-}, etc.) occupying the interlayer spacing (Al-Ghoul et al. 2010). It has also been reported that the interlayer spacing may be varied by controlling the anions between its layers, thereby having a great effect on the electrochemical activity of the particles. One of the features identified as the main difference between α- and β-$Co(OH)_2$ particles is in the orientation of their layers as β-$Co(OH)_2$ forms perfectly stacked layers along the C-axis without any intercalated ions, whilst the α-phase $Co(OH)_2$ is made up of randomly-orientated layers separated by intercalated water molecules bonded to the hydroxyl groups by hydrogen bonds (He et al. 2004). The basal plane spacing is then dependent on the intercalated species.

One of the major issues with α-$Co(OH)_2$ is the fact that it is thermodynamically metastable and may rapidly transform to β-$Co(OH)_2$ during synthesis or when it comes in contact with a strong alkali, as was the case in which the transformation of α-$Co(OH)_2$ to cobalt compounds β-$Co(OH)_2$, CoOOH and Co_3O_4 upon exposure to an alkaline medium (KOH solution) for 1–6 days (Cheng et al. 2014). The α-$Co(OH)_2$ particles also exhibit low crystallinity and a disordered structure (Al-Ghoul et al. 2010). Furthermore, the conversion of the α-form to the β-form is still unclear (Cheng et al. 2014). The blue/green colour of the α-phase has been attributed to the tetrahedral orientation of hydroxyl and intercalated anions bonded to Co(II), as well as some octahedral coordinated Co(II). The pink colour exhibited by the β-phase has been attributed to the octahedral symmetry of the particles, in the absence of any intercalating ions (Al-Ghoul et al. 2010; Rahbani et al. 2013). Various precursors to the final product may vary the structure of the particles synthesised. The transformation to cobalt oxide usually occurs in the literature concerning the β-phase. However, a comparison of the catalytic properties of cobalt oxide from both polymorphs has not been studied. We report in this work the comparison of the catalytic properties of cobalt oxide derived from both polymorphs.

The synthesis of nanomaterials is so sensitive that small changes may provide completely different results. This was also noted in the synthesis of Co_3O_4, in which the same precursor salts were used in alcohol media, using the gamma-ray technique and the thermal decomposition method. The gamma-ray technique provided spherical particles in alcohols with shorter alcohol chain lengths and fibres in alcohols with longer carbon chain lengths, in which the longest chain length explored was hexanol. The thermal decomposition also provided spherical particles in octanol, an alcohol with a carbon chain longer than that of hexanol (Athawale et al. 2010; Gamonchuang et al. 2016). Whilst the effect of alcohol chain length on Co_3O_4 synthesised via gamma-ray technique and thermal decomposition has been reported, the systematic study of the effect of alcohol chain lengths in hydro/solvothermal synthesis of cobalt oxide nanoparticles has not been studied. It was additionally demonstrated that minor changes within the hydrothermal synthesis of cobalt oxide may result in different morphologies with the simple adjustment of the amount of either hydrazine or H_2O_2 in the precursor solution (Kim and Huh 2011). Since reactions which are structure-sensitive are dependent on morphology, these simple changes not only affect the particles synthesised but also the effectiveness of their use.

The fact that a reduced particle size increases the active surface area leads one to deduce that the smaller the particle, the more reactive. Li et al. (2011) demonstrate this in their production of urchin-like Co_3O_4 nanoparticles, for which a larger specific surface area revealed a higher degradation efficiency in comparison to a lower specific area. However, nanocatalysts may be far more complex than this, as various other influences influence their reactivity. This is corroborated by Saputra et al. (2017) and Saputra et al. (2014) who highlighted the fact that higher nanocatalyst

activity lies in the combinative effect of higher surface area and active surface facets as opposed to the general concept that higher surface area alone produces higher catalytic ability. Other examples of these contradictions or departure from the expected norm of increase in reactivity as particle size reduces and surface area increases is demonstrated with cobalt oxide particle size which when in the range of 6–200 nm produces no significant improvement on the Fischer–Tropsch process but when made lower than 6 nm, exhibits inferior reactivity instead of an enhanced reactivity (Vinod 2010).

Contradicting outcomes on the effect of calcination temperature on particle size have been demonstrated wherein an increase in particle size was observed with an increase in calcination temperature for cobalt oxide particles synthesised mechanochemically, whereas a decrease in particle size was observed with increasing calcination temperature for Co_3O_4 particles synthesised by calcining $CoCO_3$ precursors prepared via solvothermal synthesis (Yang et al. 2004; Jing et al. 2012). Yang et al. (2007) investigated the effect of pH on shape-controlled nanocubic Co_3O_4 particles. During their investigation, various agents were used to maintain the pH either between 8 and 9 or between 11 and 12. Their findings showed that controlled nanocubes are formed when the pH is between 8 and 9, but irregular shapes formed at higher pH. This was attributed to the ease in condensation of the $Co(OH)_2$ precursor at higher pH values, leading to agglomeration. The results obtained by Yang et al. (2007) were reiterated in an independent study by Allawdini et al. (2014). Seeing that differences in types of reaction media, differences in their concentrations, pH, synthesis methods and protocols, etc., tend to influence the type of nanomaterials produced for the same precursor material, we undertook in this study to investigate the effect that alcohols of varying alcohol chain lengths as well as the effect of anion have on the hydro/solvothermal synthesis of cobalt oxide nanoparticles.

Anipsitakis and Dionysiou (2003) studied the degradation of organic contaminants in water using sulphate radicals produced from peroxymonosulphate, activated by cobalt in comparison to the Fenton reagent ($Fe(II)/H_2O_2$)-hydroxyl radical-based process. It was shown that at high pH values, the cobalt/peroxymonosulphate (Co/PMS) reagent maintained its degradation quality, deduced that, given sufficient reaction time, the Co/PMS system provides better degradation, even at a pH which favours Fenton reagent reactions. Subsequently, many studies have been published to evaluate the efficiency of cobalt oxide. Subsequently, much work has been done to synthesise Co_3O_4 for the evaluation of its efficiency in this process (Chen et al. 2008, Ding et al. 2012, Shi et al. 2012, Supatra et al. 2013 and Chowdhury et al. 2015). All the authors used a cobalt nitrate precursor salt ($Co(NO_3)_2{\cdot}6H_2O$ or $Co(NO_3)_2$, except Chowdhury et al. (2015) who used $CoCl_2{\cdot}6H_2O$. The test conditions, PMS concentration and pollutants varied and degradation times from 4 h to 2 min were noted. From the results presented by the authors, the Co_3O_4 synthesised from $CoCl_2{\cdot}6H_2O$ gave complete degradation in 2 min which is remarkable. However, no one has done a comparative study of the Co_3O_4 performance based on the precursor salt used.

This study therefore evaluated the effects of the precursor anion and alcohols on the cobalt hydroxide phase, the effect of calcination temperature on the resulting cobalt oxide particles, and finally the catalytic effects of the resultant Co_3O_4 particles on the colour degradation of methylene blue which is a well-known model pollutant. All experiments were conducted in 2018 and 2019 at the Cape Peninsula University of Technology (District Six Campus) in Cape Town, South Africa.

Materials and methods

Cobalt hydroxide synthesis

All chemicals used were of analytical grade and used without any further purification. For these experiments, two cobalt salts were used, namely cobalt chloride hexahydrate and cobalt nitrate hexahydrate for the hydro/solvothermal synthesis of Co_3O_4. These salts were dissolved in the solvent, which was either methanol, ethanol, propanol, butanol or octanol, or in alcohol/water solutions in the ratio 1:1. A molarity of 0.23 M was maintained for both salts. Once dissolved, the pH of the solution was adjusted to 8.10 by adding ammonium hydroxide solution dropwise. The resulting mixture was then inserted into a 0.99 L Teflon-lined pressure reactor fitted with a thermocouple and a self-regulating heating jacket. The reaction temperature was maintained at 105 ± 5 °C for 6 h after a ramp-up time of 1 h. The pressure reactor was then allowed to cool down naturally overnight. The resulting blue/green or pink suspensions were centrifuged and rinsed several times with deionised water and finally with ethanol, and dried overnight in an oven at 60 °C. Porcelain crucibles were used to store the powders, which were then annealed in a furnace at 300 °C. A standard ramp time of 1 h was used, and the set temperature was maintained for 3 h. The samples were removed immediately and stored in airtight sample vials for further analysis and application.

Characterisation

The synthesised particles were identified and tested for purity via X-ray diffraction (XRD) and Fourier transform infrared (FT-IR) spectroscopy. The XRD measurements were performed using a multipurpose BRUKER AXS D8 ADVANCE X-Ray Diffractometer fitted with

a Cu Kα monochromator, operating on a wavelength $\lambda = 1.540315$ nm, at 40 kV and 40 mA, in locked coupled, continuous scan mode. FTIR spectra were collected using a Perkin Elmer 1000 series FTIR spectrometer, operated in the range 4000–200 cm^{-1}. The morphology of the particles was analysed using an FEI Tecnai G2 20 field-emission gun (FEG) TEM, operated in bright field mode at an accelerating voltage of 200 kV, and 5 kV for SEM. Alongside SEM, Electron Dispersive X-Ray Spectroscopy (EDS) was used for quantitative elemental analysis to determine the level of purity of the Co_3O_4 samples employed. The BET surface area measurements were analysed using a Micromeritics TRISTAR II 3020 system, during which the samples were degassed at 150 °C for 2 h.

Degradation of methylene blue using the Co^{2+}/PMS system

The catalytic efficiency of the annealed Co_3O_4 particles in degrading a known water contaminant, methylene blue, was evaluated in a sulphate radical-based advanced oxidation process (AOP), using an in-house developed continuous reactor. A stock solution of 10 mg/L methylene blue solution was prepared and kept for test work. Peroxymonosulphate (Oxone®) powder of 0.184 g was added to 500 ml methylene blue solution and stirred for 5 min. An initial sample of the dye solution, along with 4 mL aliquots every 2 min at the exit of the reactor was then taken, and analysed using a handheld Lovibond® spectrocolorimeter. The spectrocolorimeter provides a numerical output (ΔE), quantifying the colour variance to a selected standard. In this case, deionised water was selected as the standard as the objective was to get the water as clear as possible. The percentage degradation was calculated as follows:

$$\%\text{Degradation} = \left(\frac{1 - \Delta E_{(\text{sample})}}{\Delta E_{(\text{deionised water})}}\right) \times 100$$

The solution was then pumped through filters filled with 0.3 g of the synthesised catalyst, in the reactor, at a flow rate of 40 ml/min using a peristaltic pump. The details of the continuous reactor and the preparation of these filters may not be disclosed as it is protected intellectual property. Samples were taken every 2 min from the start of the reaction over a period of 10 min for colour measurement.

Results and discussion

The effect of alcohols, Cl^- and NO_3^- anions on cobalt complexes, $Co(OH)_2$ and Co_3O_4

Cobalt complexes

$CoCl_2{\cdot}6H_2O$ and $Co(NO_3)_2{\cdot}6H_2O$ dissolved in water both produced pink cobalt complexes ($[Co(H_2O)_6]^{2+}$) from which green α-$Co(OH)_2$ precipitates were obtained. This reaction in water suggests that neither Cl^- nor NO_3^- has an effect on the complexation or the phase of cobalt hydroxide formed as no difference in the complex and the precipitate formed was observed. The predominant role in complexation here is therefore likely played by the H_2O molecules (Petkova and Nedkov 2013). When dissolved in 100% alcohol, the $CoCl_2{\cdot}6H_2O$ formed a blue cobalt complex and pink β-$Co(OH)_2$ precipitate, as opposed to $Co(NO_3)_2{\cdot}6H_2O$ dissolved in 100% alcohol which still gave rise to a pink coloured complex from which green α-$Co(OH)_2$ was obtained. For $CoCl_2{\cdot}6H_2O$, the change in colour of the complex from red to blue, upon a change in solvent from water to 100% alcohol, shows that the alcohol has an effect on the complexation of $CoCl_2{\cdot}6H_2O$. This is however not the case with $Co(NO_3)_2{\cdot}6H_2O$ which still forms a pink complex and green α-$Co(OH)_2$ even when the solvent is changed from water to 100% alcohol then 50% alcohol/water, indicating that the change of solvent has no effect on the complexation of $Co(NO_3)_2{\cdot}6H_2O$. $CoCl_2{\cdot}6H_2O$ dissolved in 50% alcohol/water, formed a pink cobalt complex, and a green α-$Co(OH)_2$ precipitate which turned to β-$Co(OH)_2$ over time. The change in complexation colour of $CoCl_2{\cdot}6H_2O$ from blue to pink, upon change of solvent from 100% alcohol to 50% alcohol/water, a change which is not observed with $Co(NO_3)_2{\cdot}6H_2O$, clearly points to the fact that it is primarily the alcohol and not the Cl^- and NO_3^- anion that affects complexation.

Cobalt hydroxide crystallinity and phase determination via X-ray diffraction analysis

Figure 1 presents the cobalt hydroxide powders obtained after hydro/solvothermal treatment of the pink and green cobalt complexes, respectively. Cobalt hydroxide, the precursor to cobalt oxide, exists as polymorphs alpha (α) and beta (β) cobalt hydroxide ($Co(OH)_2$) most obviously recognised by their colours green/blue and pink, respectively (Al-Ghoul et al. 2010). For cobalt complexes obtained from either $CoCl_2{\cdot}6H_2O$ and $Co(NO_3)_2{\cdot}6H_2O$ in water which were both pink, green powders were obtained. The XRD results indicated that the green powder was

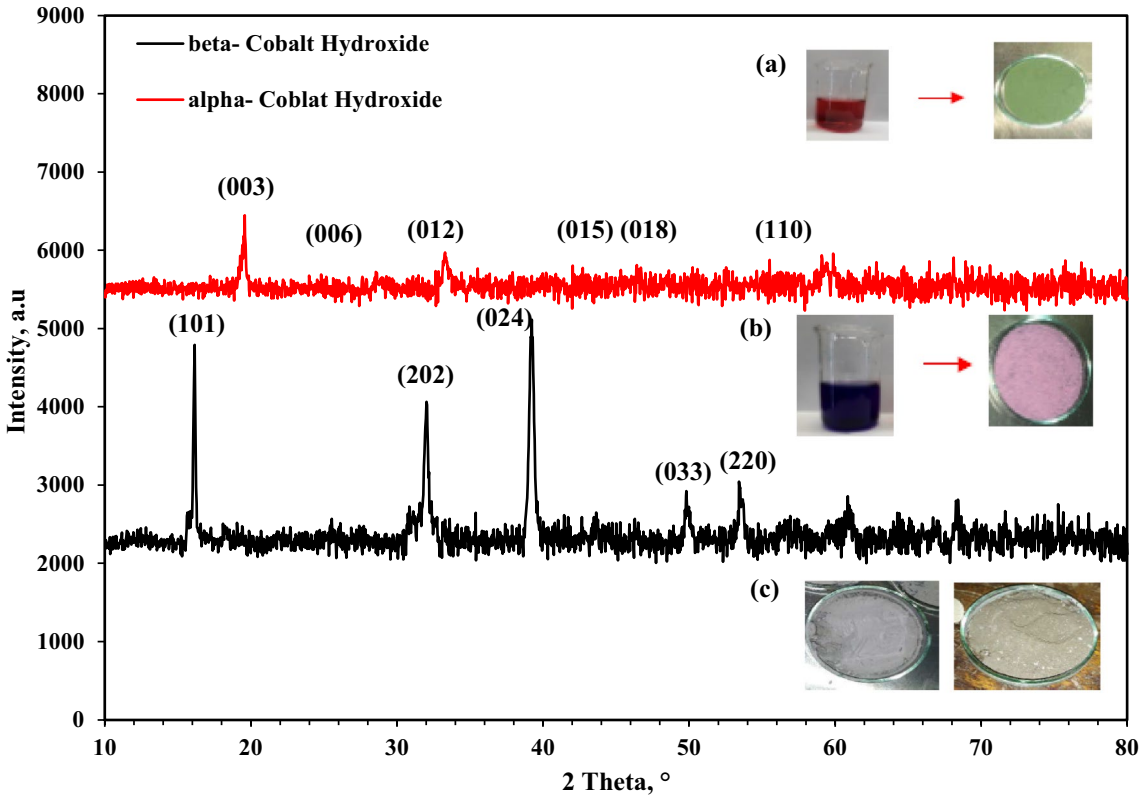

Fig. 1 $Co(OH)_2$ precursors resulting from **a** $Co(NO_3)_2{\cdot}6H_2O$ in 100% alcohol and 50% alcohol/water mixtures for both precursor salts, **b** $CoCl_2{\cdot}6H_2O$ in 100% alcohols, **c** $CoCl_2{\cdot}6H_2O$ in 50% ethanol and 50% butanol, respectively

α-$Co(OH)_2$, showing the layered double hydroxide characteristic peak (003) (Fig. 1a). The slightly broad nature of the peaks which are reflections from the (003), (006), (012), (015), (018) and (110) planes further confirm, as shown by Al-Ghoul et al. 2010, the formation of semi-amorphous α-$Co(OH)_2$. Therefore, in water only, the role of the anion on the phase of hydroxide polymorph is negligible, as only α-$Co(OH)_2$ was formed. The α-$Co(OH)_2$ phase has a layered double hydroxide structure, with positively charged layers separated by anions and water molecules (Mishra et al. 2018; Hu et al. 2009). The predominantly tetrahedral coordinated Co (II) ions, along with the intercalated anions (Cl^-, NO_3^-, OH^-) and water molecules, provide a large interlayer spacing of > 0.7 nm and disordered structure, which cause the green/blue colour of α-$Co(OH)_2$ (Al-Ghoul et al. 2010). For $CoCl_2{\cdot}6H_2O$ in 100% alcohols, only pink, more crystalline β-$Co(OH)_2$ was formed. This was confirmed by the XRD spectrum (Fig. 1b), for which characteristically sharp peaks, representing reflections from the (101), (003), (202), (024), (033) and (220) planes were observed similar to that of Al-Ghoul et al. (2010). The pink coloured β-$Co(OH)_2$ consists of octahedrally coordinated Co(II) ions, with their perfectly ordered stacking along the C-axis, and an interlayer spacing of 0.46 nm in which is absent intercalated anions and water molecules (Al-Ghoul et al. 2010; Rahbani et al. 2013). The remainder of the $CoCl_2{\cdot}6H_2O$ and $Co(NO_3)_2{\cdot}6H_2O$-derived complexes mostly produced green α-$Co(OH)_2$ powders, with the exception of $CoCl_2{\cdot}6H_2O$ in 50% ethanol and 50% butanol, which initially produced green precipitates that were converted to grey/brown powders (Fig. 1c). It has been reported that α-$Co(OH)_2$ is thermodynamically metastable and may therefore rapidly transform to β-$Co(OH)_2$ during synthesis or in contact with a strong alkali (Al-Ghoul et al. 2010; Rahbani et al. 2013). From this, one might assume that the 50% ethanol and 50% butanol samples shown in Fig. 1c contain both α-$Co(OH)_2$ and β-$Co(OH)_2$. This was, however, not the case as XRD only pointed solely to the presence of the β-$Co(OH)_2$. This is probably an indication that under these synthesis conditions, a structurally different form of β-$Co(OH)_2$ was produced that does not have the expected pink colour. This may find useful applications if further investigated.

The XRD plot in Fig. 2 shows that essentially Co_3O_4 was obtained from both α- and β-cobalt hydroxide polymorphs emanating from $CoCl_2.6H_2O$ and $Co(NO_3)_2{\cdot}6H_2O$ precursors dissolved in 100% alcohol (methanol, ethanol,

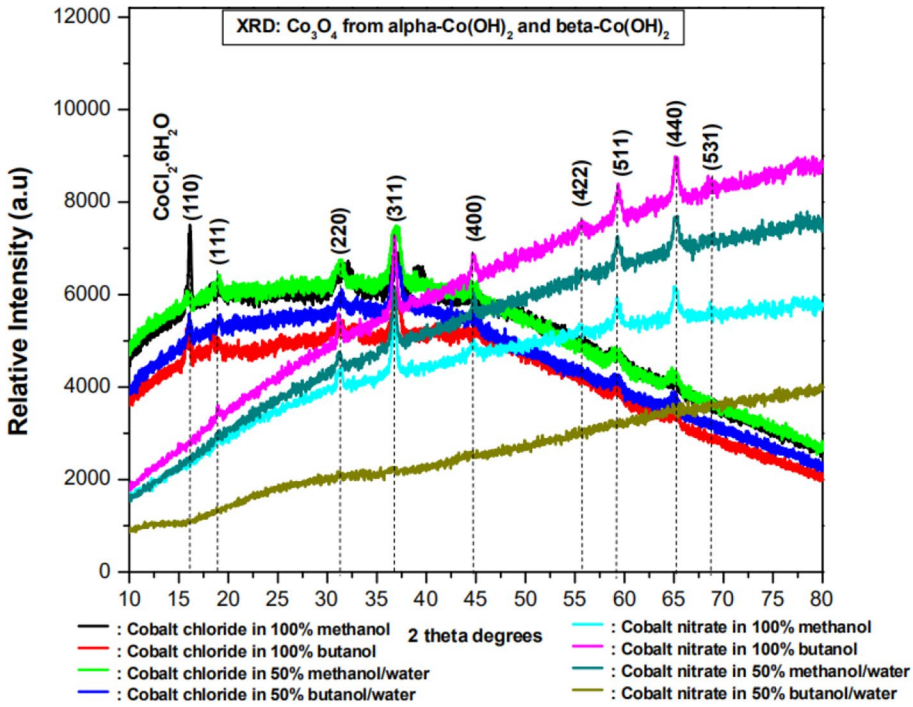

Fig. 2 XRD spectra for the Co_3O_4 particles synthesised from $CoCl_2{\cdot}6H_2O$ and $Co(NO_3)_2{\cdot}6H_2O$ in 100% alcohol and 50% alcohol/water solutions

butanol) and 50% alcohol/water mixtures. The peaks represented by XRD are in accordance with the JCPDS card 42–1467, which exhibits diffraction peaks at 19°, 31.3°, 36.9°, 38.6°, 44.8°, 55.7°, 59.4° and 65.2°, indexed to (111), (220), (311), (222), (400), (422), (511) and (440). These peaks show that Co_3O_4 from both α- and β-Cobalt hydroxide crystallises in the face-centred cubic phase. Co_3O_4 emanating from $Co(NO_3)_2{\cdot}6H_2O$-derived $Co(OH)_2$ however appears to be more crystalline with sharper peaks of higher intensity, whilst Co_3O_4 from $CoCl_2{\cdot}6H_2O$-derived $Co(OH)_2$ appears to be slightly less crystalline as is shown by the broader peaks observed. This latter form of Co_3O_4 should be more amorphous and have a smaller average crystallite and particle size and a greater surface area per gram of sample than the former (Co_3O_4 emanating from $Co(NO_3)_2{\cdot}6H_2O$-derived $Co(OH)_2$). A higher surface area should lead to better catalytic degradation performance.

XRD analysis shows the existence of impurities in Co_3O_4 from all samples emanating from $CoCl_2{\cdot}6H_2O$-derived $Co(OH)_2$. At 16°, the (110) peak can be attributed to the presence of unreacted $CoCl_2.6H_2O$, $CoCl_2{\cdot}H_2O$ (JCPDS# 00–025-0242; 00–029-0466) or $Co_2(OH)_3Cl$ (JCPDS# 01–073-2134).

Powder emanating from $Co(OH)_2$ prepared through the dissolution of $Co(NO_3)_2{\cdot}6H_2O$ in 50% butanol/water showed no peaks pointing to unusually high amorphicity after heating in air, at 300 °C.

Cobalt oxide elemental analysis and chemical bond speciation via EDS and FTIR spectroscopy

Figures 3 and 4 show the EDS and FTIR spectra of the cobalt oxide particles obtained after calcination, respectively. EDS was used to identify the elemental makeup of the samples synthesised. The peaks showed evidence of cobalt and oxygen, the constituents of the Co_3O_4. It also presented peaks for carbon and copper from the copper grid used in the analysis process. Besides these peaks, additional peaks at ± 2260 eV were evident, showing the presence of chloride ions. This can be attributed to unused $CoCl_2{\cdot}6H_2O$ or the formation of $Co_2(OH)_3Cl$. Whilst the samples synthesised from cobalt nitrate in 100% alcohols presents no impurity, the samples synthesised in 50% alcohol/water presented an impurity between 2500 and 2700 eV, which was attributed to the presence of sulphur. Quantitative EDS (Tables S1-S7) confirmed the presence of Cl in the Co_3O_4 samples derived from $CoCl_2{\cdot}6H_2O$ precursor, with Cl amounting to 1.44, 10.21 and 15 atomic % in the different samples. This corroborates the observation of a (110) peak, indexed to $CoCl_2{\cdot}6H_2O$, in XRD of the cobalt oxide samples (Fig. 2). Sulphur impurities in the range of 1–6 atomic % were observed in the Co_3O_4 derived from $Co(NO_3)_2{\cdot}6H_2O$ precursors. The presence of sulphur in these samples is explained by the presence of sulphates (0.005%) in the $Co(NO_3)0.6H_2O$ precursors.

The FTIR spectra for the Co_3O_4 particles (Fig. 4) synthesised from $CoCl_2{\cdot}6H_2O$ in 100% alcohol, $CoCl_2{\cdot}6H_2O$

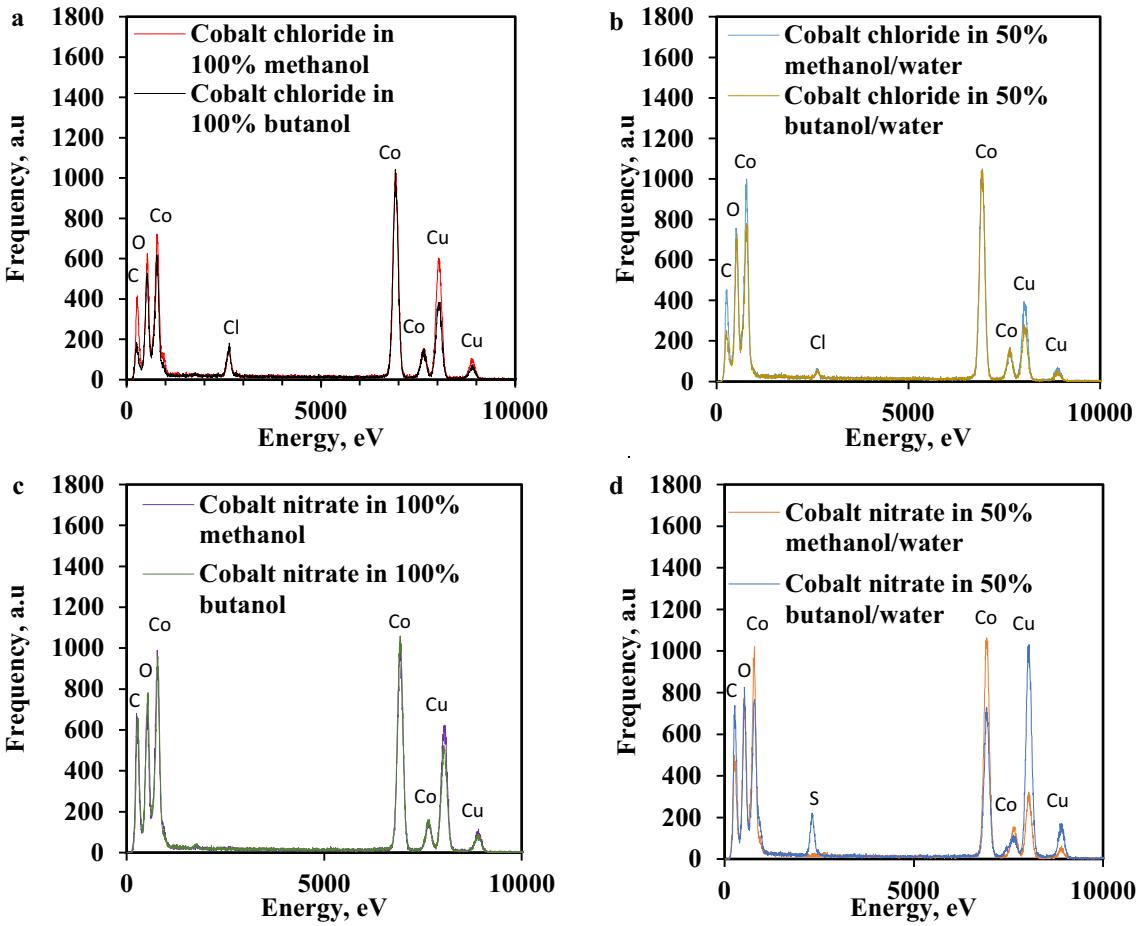

Fig. 3 EDS spectra for the Co_3O_4 particles synthesised from **a** $CoCl_2{\cdot}6H_2O$ in 100% alcohol, **b** $CoCl_2{\cdot}6H_2O$ in 50% alcohol/water solutions, **c** $Co(NO_3)_2{\cdot}6H_2O$ in 100% alcohol and **d** $Co(NO_3)_2{\cdot}6H_2O$ in 50% alcohol/water solutions

in 50% alcohol/water, $Co(NO_3)_2{\cdot}6H_2O$ in 100% alcohol, and $Co(NO_3)_2{\cdot}6H_2O$ in 50% alcohol/water solutions all exhibit strong peaks in the 550–660 cm^{-1} range that can be ascribed to bending vibrations in Co_3O_4 (Chani et al. 2015). Additional peaks at 3460 cm^{-1} and 1600 cm^{-1} are attributed, respectively, to the broad peak of OH stretching bonds in water, and surface adsorbed moisture. For cobalt oxide particles synthesised from $Co(NO_3)_2{\cdot}6H_2O$ in 50% alcohol/water solutions an additional peak at 1100 cm^{-1} which can be attributed to the presence of $CoSO_4$ (Ariponnammal et al. 2020) was noted.

From the XRD spectra especially, and in conjunction with EDS and FTIR, it is evident that regardless of the cobalt hydroxide polymorph obtained, cobalt oxide is formed during the calcination process.

Cobalt oxide shape and particle size determination via SEM and TEM

The TEM images provided in Fig. 5 show that the $CoCl_2{\cdot}6H_2O$ in water, as a precursor, produced cobalt oxide particles which were rod shaped and approximately 30 nm in size, whilst the $Co(NO_3)_2{\cdot}6H_2O$ in water produced agglomerated particles. Subsequent SEM images showed that these agglomerates were 20 µm in size. $CoCl_2{\cdot}6H_2O$ in alcohols at both 100% and 50% concentrations produced diamond shapes, approximately 50 nm in size. The $Co(NO_3)_2{\cdot}6H_2O$ precursor in alcohols at 100% and 50% concentrations mostly produced nanorods, resembling the particles formed from $CoCl_2{\cdot}6H_2O$ in pure water, apart from instances in which an amorphous state was observed.

The particle size was determined from the TEM images (Fig. 5), measuring an average of 200 particles using ImageJ© software. The diameters are based on the diagonal length of diamond shapes and the length of the rod shapes, as shown in Fig. 5. The particle size distributions were dominated by the anion rather than the alcohol. Narrow size distributions were obtained in the presence of nitrate for all alcohol and alcohol/water solutions, in contrast to the wide particle size distributions obtained in the presence of chlorides (Fig. 6). Table 1 shows that the average particle size increase with alkyl chain length, independent of

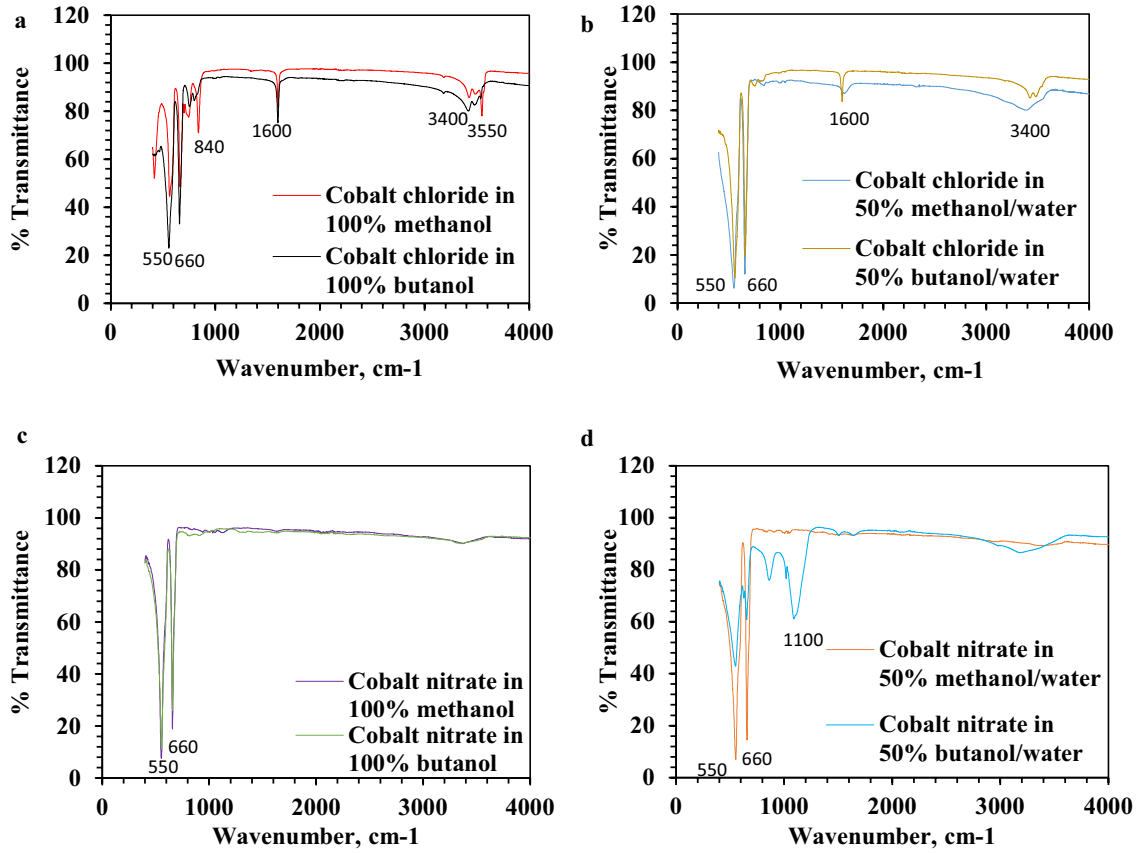

Fig. 4 FT-IR spectra for the Co_3O_4 particles synthesised from **a** $CoCl_2{\cdot}6H_2O$ in 100% alcohol, **b** $CoCl_2{\cdot}6H_2O$ in 50% alcohol/water solutions, **c** $Co(NO_3)_2{\cdot}6H_2O$ in 100% alcohol and **d** $Co(NO_3)_2{\cdot}6H_2O$ in 50% alcohol/water solutions

the anion, with the exception of octanol where the particle size decreased. Generally, in comparison to the 100% alcohol solutions, the 50% alcohol solutions resulted in smaller particles for cobalt chloride and cobalt nitrate hexahydrate precursors (Table 2).

Evaluation of the cobalt oxide particles synthesised as catalysts in colour degradation

Comparison of $CoCl_2{\cdot}6H_2O$- and $Co(NO_3)_2{\cdot}6H_2O$-derived Co_3O_4 particles

The degradation curves presented in Fig. 7a and b show the treatment of a 500 ml sample of methylene blue over a period of 10 min, using the cobalt oxide particles synthesised from $CoCl_2{\cdot}6H_2O$ in either water, 100% or 50% alcohols, respectively, to activate PMS. An initial sample (Fig. 7a) was taken, along with samples every 2 min from the start of the reaction. From the results shown in Fig. 7a, it may be seen that the particles produced from 100% alcohols have a higher degradation rate resulting in a product with no visible colour than that of the particles synthesised in the 50% alcohol solutions and water only. The particles synthesised from $Co(NO_3)_2{\cdot}6H_2O$ in 100% and 50% alcohols, respectively, are shown in Figs. 7c and d. It is noted that within 10 min of treating the methylene blue solutions, less than 10% degradation occurred for all the samples synthesised in 100% alcohol, whilst the cobalt oxide particles synthesised in 50% alcohol performed at better degradation rates, with the lowest degradation being 4.2% for the pure water sample and the highest degradation being 91.3% for the cobalt oxide particles synthesised in 50% propanol solution. The $CoCl_2{\cdot}6H_2O$-derived Co_3O_4 particles performed better when synthesised in 100% alcohol, whilst the $Co(NO_3)_2{\cdot}6H_2O$-derived Co_3O_4 particles performed better when synthesised in 50% alcohol solutions.

Effect of particle size and impurities on catalytic performance

In Fig. 8 the catalytic activity of the catalysts at 2 min was plotted against the d_{50} particle sizes and the crystallite sizes of the most and least rapid catalyst activity achieved. From Fig. 8a, it was found that at a particle size of approximately

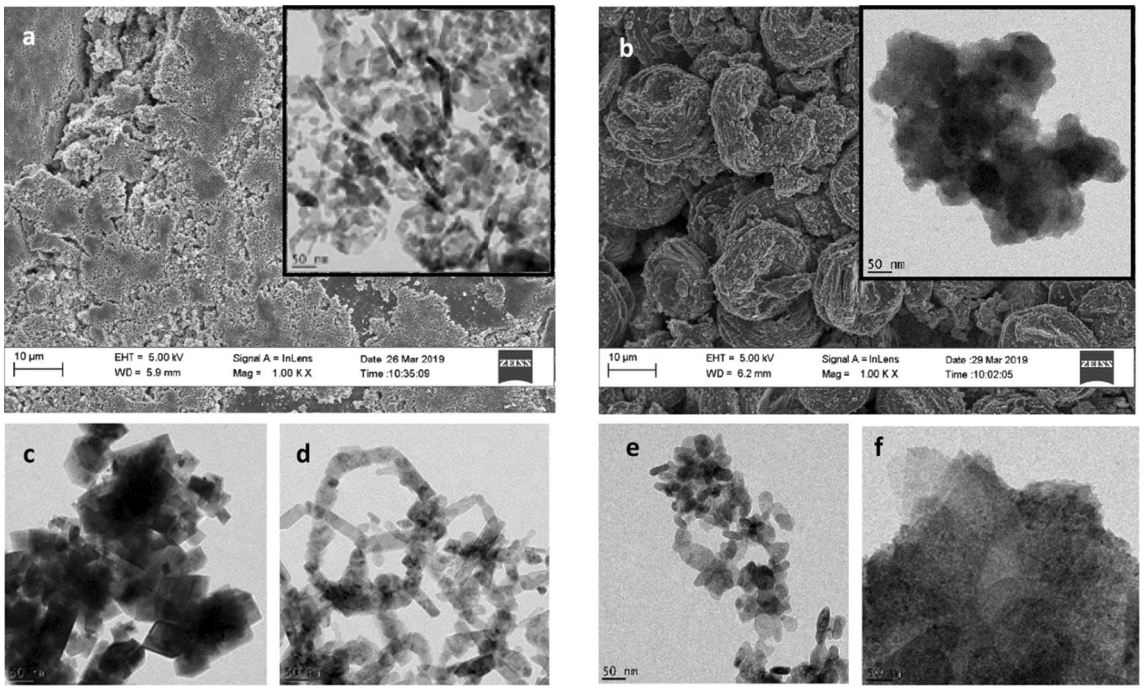

Fig. 5 TEM and SEM images for the Co_3O_4 synthesised from **a** $CoCl_2$ in water, **b** $Co(NO_3)_2$ in water, **c** and **d** TEM images of the Co_3O_4 synthesised from $CoCl_2$ in 100% and 50% methanol, respectively, and **e** and **f** TEM images of the Co_3O_4 prepared from $Co(NO_3)_2$ in 100% and 50% butanol, respectively

Table 1 Effect of the solvent medium on the complexation of $CoCl_2{\cdot}6H_2O$ and $Co(NO_3)_2{\cdot}6H_2O$

Solvent	$CoCl_2{\cdot}6H_2O$ complex colour	$Co(NO_3)_2{\cdot}6H_2O$ complex colour	$CoCl_2{\cdot}6H_2O$ phase type & colour	$Co(NO_3)_2{\cdot}6H_2O$ phase type & colour
Water	Pink	Pink	α-$Co(OH)_2$ green	α-$Co(OH)_2$ green
100% alcohol	Blue	Pink	β-$Co(OH)_2$ pink	α-$Co(OH)_2$ green
50% alcohol/water	Pink	Pink	α-$Co(OH)_2$ green	α-$Co(OH)_2$ green

Table 2 d50 particle sizes for the cobalt oxide particles, adapted from the particle size distributions

	Solvent	100% alcohol	50% alcohol
Cobalt chloride precursor	Methanol	46.79 nm	41.76 nm
	Ethanol	56 nm	46.07 nm
	Propanol	66.5 nm	33.94 nm
	Butanol	67.14 nm	54.67 nm
	Octanol	65.27 nm	22 nm
Cobalt nitrate precursor	Methanol	19.19 nm	22.67 nm
	Ethanol	24.18 nm	22.23 nm
	Propanol	34.61 nm	Amorphous
	Butanol	37.03 nm	
	Octanol	28.65 nm	

60 nm and above, the degradation rate increases rapidly, contrary to the notion that increased catalytic activity is dependent on the increased surface area.

However, degradation of only 20% occurred for the cobalt nitrate precursor samples. The particle sizes ranged between 20 and 70 nm for both the cobalt oxide synthesised from $CoCl_2{\cdot}6H_2O$ and from $Co(NO_3)_2{\cdot}6H_2O$. Highly active cobalt oxide particles had crystallite sizes between approximately 8, 5 and 11 nm for both cases. This was reiterated in the effect of calcination temperature on catalytic performance, as the crystallite sizes generally increased with increasing temperature, negatively affecting the catalytic ability. The exception to this finding further reiterated the effect of crystallite size range on high activity of cobalt oxide, as

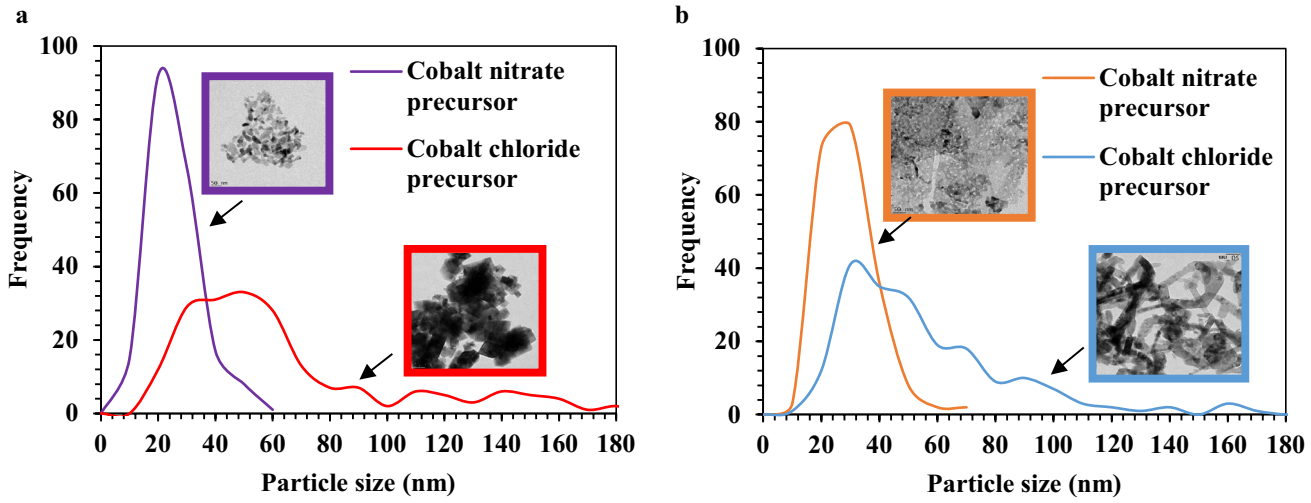

Fig. 6 PSD curves for the Co_3O_4 particles synthesised from $CoCl_2{\cdot}6H_2O$ and $Co(NO_3)_2{\cdot}6H_2O$ in various alcohols at (**a**) 100% or (**b**) 50% concentrations

the cobalt oxide synthesised from the nitrate precursor in 50% octanol experienced a crystallite decrease to 9.73 nm, consequently providing a faster degradation rate than those calcined at 300 and 400 °C. As crystallite size increases particle size increases and the surface area/g of sample reduces making smaller by proportion the amount of active sites available for catalytic degradation of methylene blue. The smaller the crystallite size the greater the surface area/g of sample available for catalysis, hence the smaller sized particles/crystallites show better catalytic degradation activity than the larger size particles/crystallites observed at increasing annealing temperatures. Table 3 shows a summary of the best performing catalysts.

In order to evaluate the role of the chloride impurity on the catalytic performance of Co_3O_4 derived from β-$Co(OH)_2$ prepared in 100% alcohol solutions (Table 3), a β-$Co(OH)_2$ sample prepared in 100% Methanol was washed several times to remove excess chloride prior to calcination. The EDS result of Co_3O_4 prepared from this thoroughly washed sample showed a drop in chloride content from 10.21 atomic % to 0.61 atomic %. Interestingly, the catalytic performance of the resultant Co_3O_4 catalyst reduced from almost 100% to only 5% degradation implying that Cl^- anions from $CoCl_2{\cdot}6H_2O$ play a significant role in the catalytic performance of the Co_3O_4 catalysts prepared from $CoCl_2{\cdot}6H_2O$ precursors. This enhancing effect of $CoCl_2{\cdot}6H_2O$ on the catalytic performance of Co_3O_4 has been reported by Hao et al (2016). It is worth noting, however, that a phase change from pink β-$Co(OH)_2$ to green α-$Co(OH)_2$ was also observed at the end of the rigorous washing process carried out to remove the chlorides. This phase change clearly suggests that Cl^- anions do play a significant role in the formation of the β-$Co(OH)_2$ phase. The XRD results in Fig. 2 shows the presence of Cl^- anions in all the $CoCl_2{\cdot}6H_2O$-derived Co_3O_4 in 100% and 50% alcohol solutions, yet and degradation results in Fig. 7a-b shows that Co_3O_4 derived in 100% alcohol solutions performed superior to those in 100% alcohol. Table 1 shows that α-$Co(OH)_2$ was formed when using 50% alcohol solutions and β-$Co(OH)_2$ in 100% alcohol. The drastic reduction in the catalytic performance of the rigorously washed $Co(OH)_2$-derived Co_3O_4 suggests rather strongly that the type of $Co(OH)_2$ phase from which the Co_3O_4 is derived influences its catalytic degradation performance rather than the Cl^- impurity itself. Concerning the occurrence of sulphur and its role in the performance of Co_3O_4 derived from $Co(NO_3)_2{\cdot}H_2O$ in 50% butanol, repeat synthesis of this α-$Co(OH)_2$ and its subsequent calcination was carried out. EDS showed a similar sulphur content of 8.5 atomic % compared to the initial 6.5 atomic %. A similar degradation profile was observed within the first 2 min with a progressive drop in performance in a subsequent 8 min. From the less than stable degradation observed with this repeat Co_3O_4 sample prepared from $Co(NO_3)_2{\cdot}H_2O$ in 50% butanol, the case of a threshold limit on the amount of S impurity needed in the Co_3O_4 catalyst can be made. These repeatability tests showed clearly that S in the samples was not a product of cross-contamination in the reactor. The presence of sulphur could therefore be retraced to the sulphate content (0.005%) in the commercial $Co(NO_3)_2{\cdot}6H_2O$ precursor (B&M Scientific).

Comparison with commercially available Co_3O_4

Commercially available Sigma-Aldrich cobalt oxide at sizes 50 nm and at 10 µm was selected to comparatively assess the catalytic activity of the cobalt oxide particles

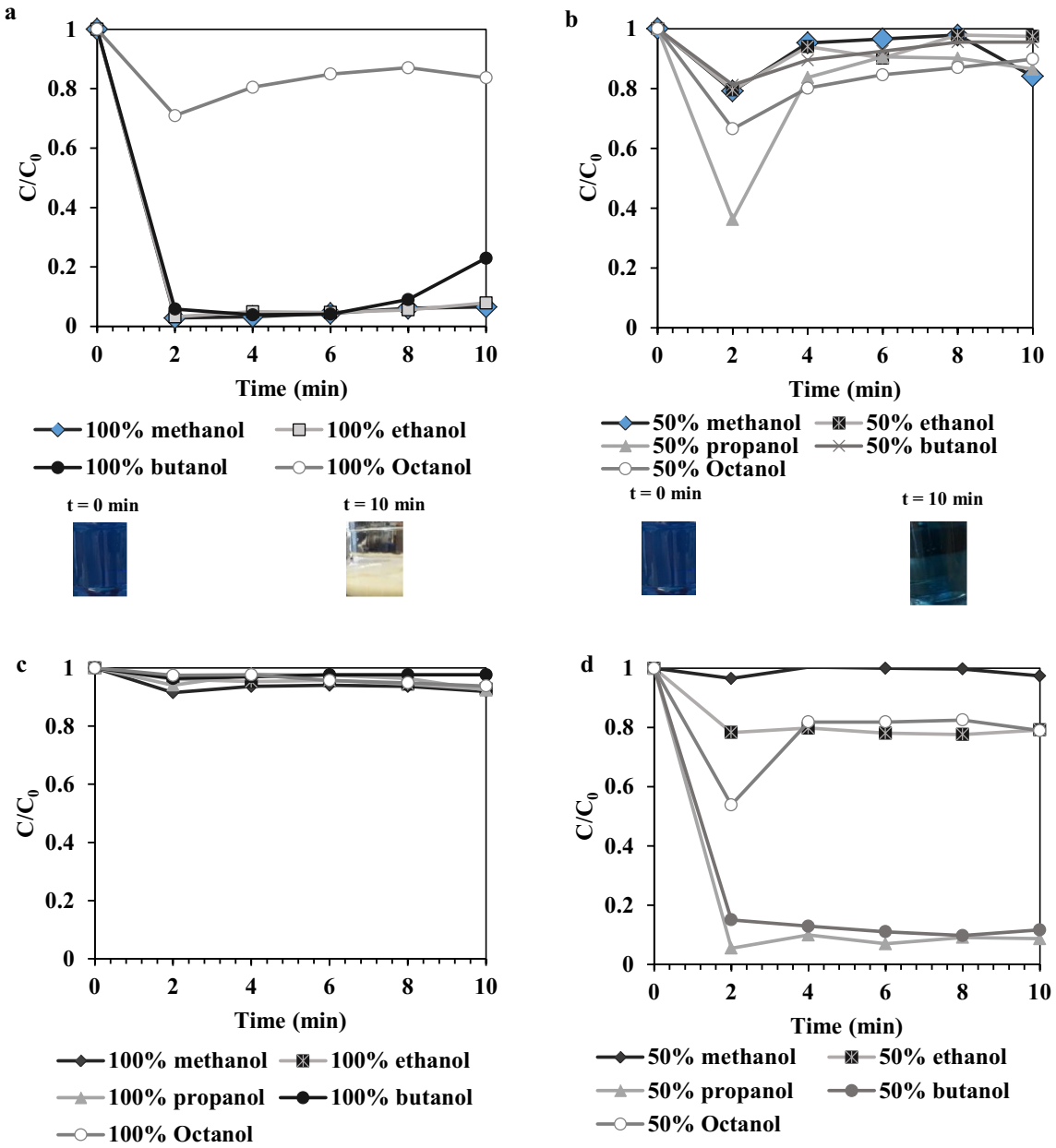

Fig. 7 Degradation curves for the methylene blue solutions degraded using the Co_3O_4 catalysts synthesised from **a** $CoCl_2{\cdot}6H_2O$ in 100% alcohols, **b** $CoCl_2{\cdot}6H_2O$ in 50% alcohol/water solutions, **c** $Co(NO_3)_2{\cdot}6H_2O$ in 100% alcohols and **d** $Co(NO_3)_2{\cdot}6H_2O$ in 50% alcohol/water solutions, calcined at 300 °C

synthesised. Figure 8 shows both that the performance of the commercially available samples provided a degradation quality similar to the worst performing cobalt oxide synthesised from $CoCl_2{\cdot}6H_2O$ in 50% ethanol and $Co(NO_3)_2{\cdot}6H_2O$ in 100% butanol. The cobalt chloride in 100% methanol and cobalt nitrate in 50% propanol solution provided the best degradation, and exceeded the degradation quality of the commercially available cobalt oxide by 85%. The enhancing role of the Cl and S impurities on the catalytic performance of the Co_3O_4 as previously discussed is clearly highlighted with these Co_3O_4 samples which show no Cl and S contamination under quantitative EDX analysis. As observed in Fig. 9 and S8-9, repeat evaluation of the highly pure commercial Co_3O_4 samples from Sigma Aldrich for catalytic degradation of Methylene Blue in the presence of Oxone, and subsequent comparison to our prepared Cl and S-containing Co_3O_4 samples shows a distinctly poor performance (< 10% degradation) for the commercial Co_3O_4 as opposed to > 90% for our prepared samples. In the case

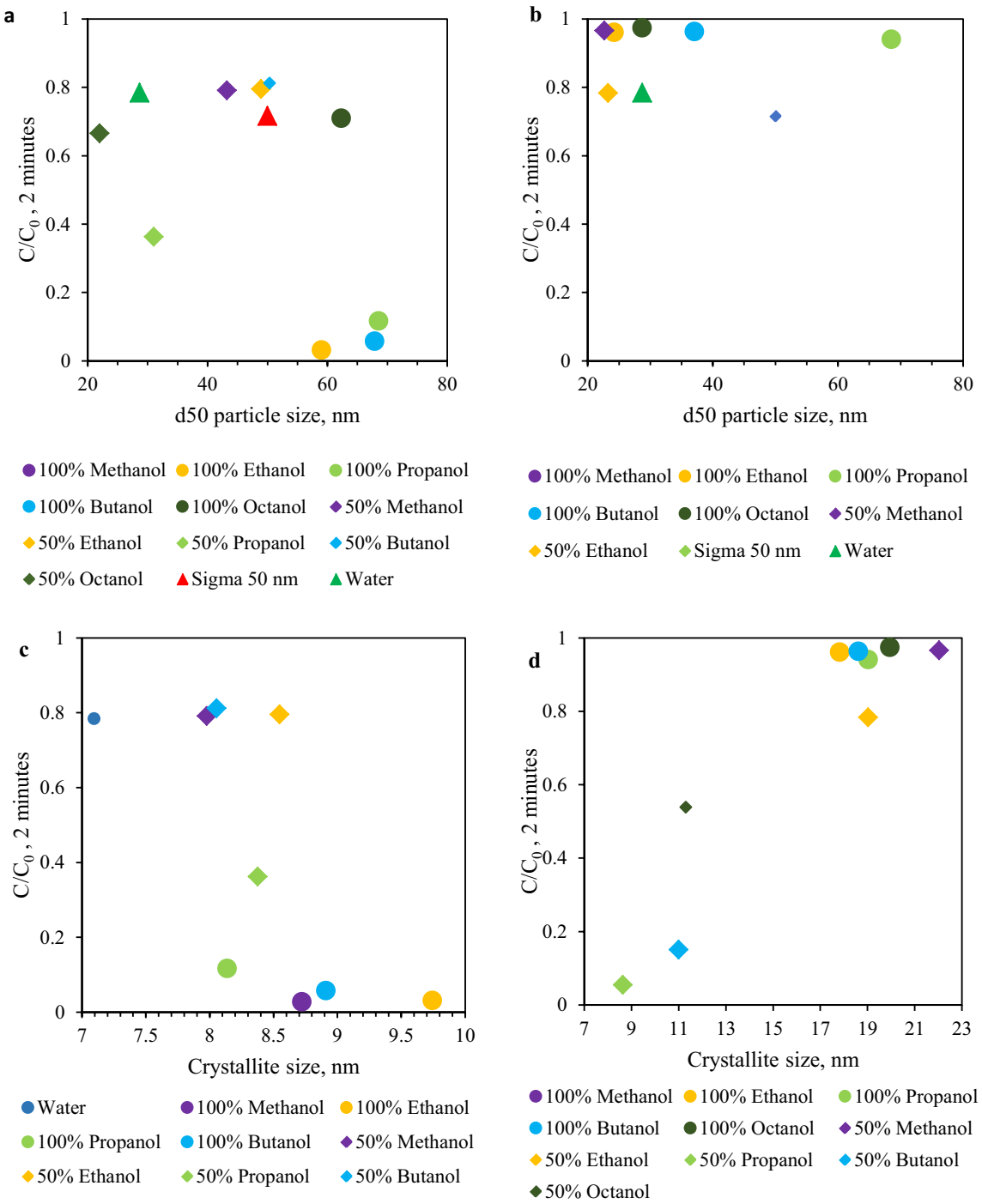

Fig. 8 Degradation quality at 2 min vs. d50 particle size for the particles synthesised from **a** $CoCl_2{\cdot}6H_2O$ and **b** $Co(NO_3)_2{\cdot}6H_2O$ in 100% and 50% alcohol solutions, and degradation quality at 2 min vs. crystallite size for the particles synthesised from **c** $CoCl_2{\cdot}6H_2O$ and **d** $Co(NO_3)_2{\cdot}6H_2O$ in 100% and 50% alcohol solutions

of the commercially available Co_3O_4, it is not possible to establish whether it was produced from α-$Co(OH)_2$ or β-$Co(OH)_2$ to test our hypothesis.

Optimisation of process conditions for best performing Co_3O_4

Optimisation studies were performed on the sample showing the highest degradation rate; the cobalt oxide particles

Table 3 Summary of best performing catalysts

Cobalt salt	Solvent	Complex colour	Hydroxide polymorph	Hydroxide colour	Oxide	Impurities EDS	Impurities XRD	FWHM crystallite (nm)	D_{50} TEM (nm)	BET m^2/g
$CoCl_2{\cdot}6H_2O$	100% Methanol	Blue	β	Pink	Co_3O_4	Cl	Cl	8.72	46	13
$CoCl_2{\cdot}6H_2O$	100% Ethanol	Blue	β	Pink	Co_3O_4	Cl	Cl	9.74	56	23
$Co(NO_3)_2{\cdot}6H_2O$	50% Proponol/water solution	Pink	α	Green	Co_3O_4	S	–	8.64	Semi-armor-phous	12
$Co(NO_3)_2{\cdot}6H_2O$	50% Butanol/water solution	Pink-	α	Green	Co_3O_4	S	–	11.0	Semi-armor-phous	12

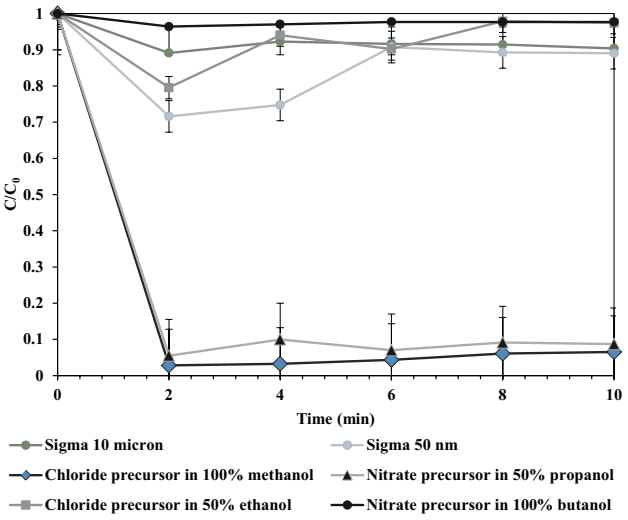

Fig. 9 Degradation curves for the methylene blue solutions using commercial and synthesised Co_3O_4

synthesised from cobalt chloride precursor salt in 100% methanol, calcined at 300 °C. The effectiveness of these particles was evaluated and optimised using the methylene blue degradation process. As shown in Fig. 10, these factors included: the catalyst load on filter, the Oxone concentration, and filter bed thickness. The best conditions were used to treat higher concentrated methylene blue solutions. Firstly, the catalyst load was changed from 0.15 g to 0.4 g per filter and it was found that a catalyst load showing the fastest degradation rate was that of 0.3 g. The 0.2 g load, however, provided very similar results and would be more viable from a cost standpoint. Using the most effective catalyst load and maintaining it, the Oxone concentration was varied. As shown in Fig. 10, concentrations were increased by 0.093 g per 500 ml of methylene blue treated. The highest degradation was provided by an Oxone concentration of 0.184 g. The concentration of 0.367 g provided the second highest degradation. This shows that a concentration of 0.184 g Oxone is not only preferable for degradation rate, but also for cost analysis. Increased concentrations at 50, 75 and 100 mg/L were treated using the best catalyst load and Oxone concentrations. The 50 mg/L concentrated methylene blue solution was degraded by 95.4% using the same conditions, and an increase to 75 mg/L and 100 mg/L displayed a major drop in degradation as they were only degraded by 35.5% and 11.82%, respectively. The possibility that an increased catalyst surface area over a larger filter bed, made up of three individual filters stacked on one another, would increase the degradation of the higher concentrated dye was investigated. From the investigation, it was found that no substantial changes were made for the increased dye concentration of 75 mg/L to account for the increased cost of making more filters. These findings are important, as they

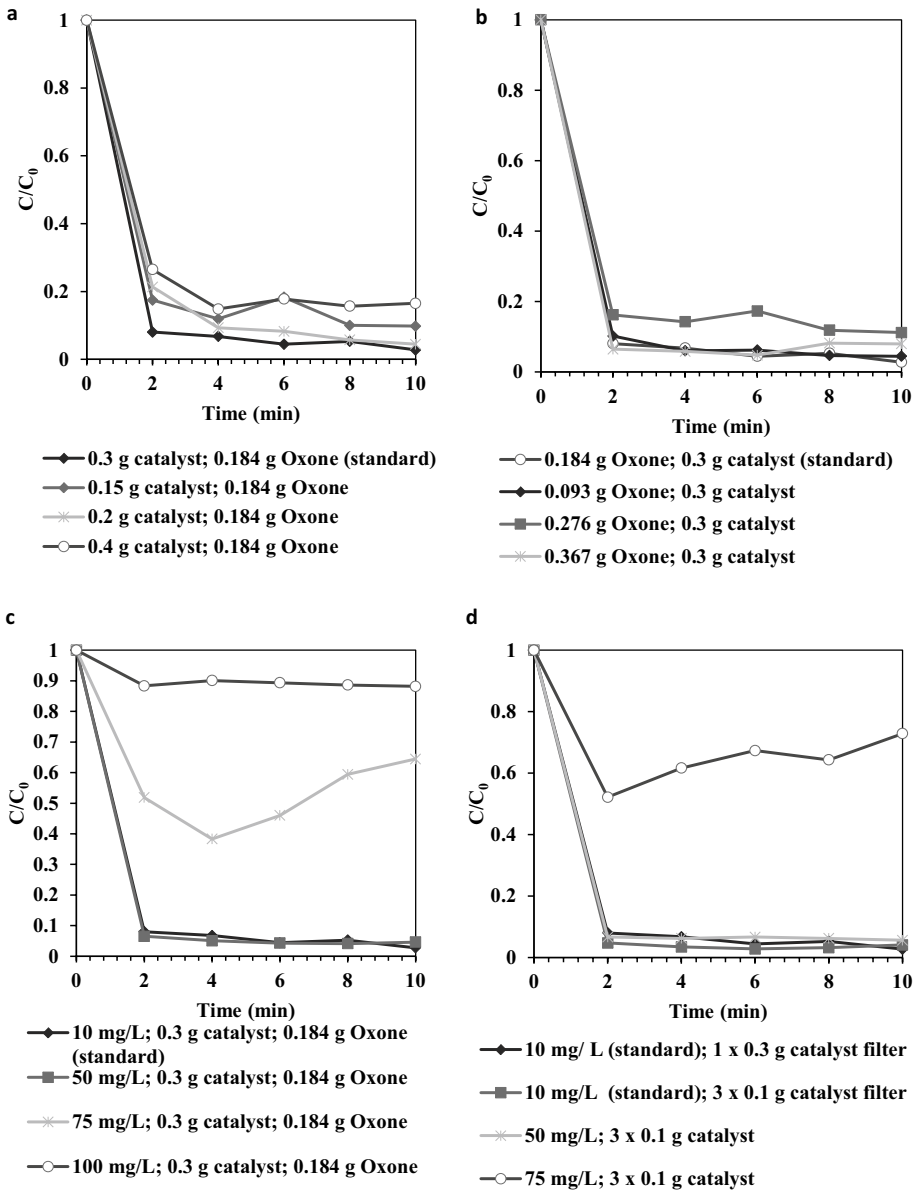

Fig. 10 Methylene blue degradation with **a** catalyst load variation, **b** Oxone variation, **c** dye concentration and **d** filter bed variation

provide a starting point for the treatment of actual textile wastewater using these methods.

Conclusion

This study provides a comparison of the chloride and nitrate anions in the formation of cobalt complexes and its subsequent effect on the cobalt hydroxide polymorph and cobalt oxide formed. This research found that only pink octahedral cobalt complexes are formed from cobalt nitrate salts, whether in 100% alcohol solutions or in water or 50% alcohol/water solutions, differing from the cobalt chloride salt which has been established to provide pink complex solutions in water and blue complex solutions in alcohols. Shape and size variances occurred for the change in anion used, whilst the use of various alcohols maintained the shape and approximate size of the particles. The chloride-based particles generally produced rhombic-shaped cobalt oxide nanoparticles approximately 50 nm in size, with the exception of the water and 50% methanol batch, which produced nanorods. The nitrate-based particles were nanorod-like particles, approximately 30 nm in size, as measured from the TEM images. The particle size distributions were dominated by the anion (whether Cl^- or NO^-_3) rather than the alcohol. Narrow size distributions were obtained in the presence of nitrates for all alcohol and alcohol/water solutions, in contrast to the wide particle size distributions obtained in the presence of chlorides. It was found that the degradation of methylene blue solutions using the cobalt oxide particles

calcined from β-cobalt hydroxide provided better degradation than those calcined from α-cobalt hydroxide. However, when impurities like S exist in cobalt oxide samples produced from the nitrate precursor salts, their performance noticeably improved.

Further investigation of this phenomena is required to enable synthesis strategies for large scale on-demand production of cobalt oxide nanoparticles for application in cobalt catalyzed sulphate radical advanced oxidation processes for wastewater treatment.

Acknowledgments We would like to acknowledge our funders for student bursary Nedbank Eyethu Trust as well as the Technology Innovation Agency of South Africa for Grant number 10022016 OC16/1538-2 | 1040/02 that provided the running cost for this project.

References

Allawdini G, Masrinda S, Pudukudy M (2014) The effect of pH on cobalt oxide nano particles synthesis. Aust J Basic App Sci 8(19):243–247

Al-Ghoul M, El-Rassy H, Coradin T, Mokalled T (2010) Reaction-diffusion based co-synthesis of stable a- and b- cobalt hydroxide in bio-organic gels. J Cryst Growth 312:856–862

Anipsitakis GP, Dionysiou DD (2003) Degradation of organic contaminants in water with sulphate radicals generated by the conjunction of peroxymonosulfate with cobalt. Environ Sci Technol 37:4790–4797

Ariponnammal S, Anusha S, Shalini S (2020) Structural and spectroscopic investigations on cobalt sulphate. Mater Proc 27(1):336–339

Athawale AA, Majumdar M, Singh H, Navinkiran K (2010) Synthesis of Cobalt Oxide nanoparticles/ fibres in alcoholic medium using gamma-ray technique. Def Sci J 60(5):507–513

Chani MTS, Khan SB, Karimov KS, Asiri AM, Akhtar K, Arshad MN (2015) Synthesis and pressure sensing properties of the pristine cobalt oxide nanopowder. Int J Electrochem Sci 10:10433–10444

Chen K, Lo S, Chang L, Egerton R, Kai J, Lin J, Chen F (2007) Valence state map of iron oxide thin film obtained from electron spectroscopy imaging series. Micron 38:354–361

Chen X, Chen J, Qiao X, Wang D, Cai X (2008) Performance of nano-Co_3O_4/peroxymonosulfate system: kinetics and mechanism study using acid orange 7 as a model compound. Appl Catal B Environ 80:116–121

Cheng JP, Liu L, Zhang J, Liu F, Zhang XB (2014) Influences of anion exchange and phase transformation on the supercapacitive properties of α-$Co(OH)_2$. J Electroanal Chem 722–723:23–31

Chowdhury M, Oputu O, Kebede M, Cummings F, Cespedes O, Maelsand A, Fester V (2015) Rapid and large-scale synthesis of Co_3O_4 octahedron particles with very high catalytic activity, good supercapacitance and unique magnetic property. RSC Adv 5:104991

Deng Y, Zhao R (2015) Advanced oxidation processes (AOPs) in wastewater treatment. Curr Pollut Rep 1:167–176

Ding Y, Zhu L, Huang A, Zhao X, Zhang X, Tang H (2012) A heterogeneous Co_3O_4-Bi_2O_3 composite catalyst for oxidative degradation of organic pollutants in the presence of peroxymonosulfate. Catal Sci Technol 2:1977–1984

El-Batlouni H, El-Rassy H, Al-Ghoul M (2008) Cosynthesis, coexistence, and self- organization of α- and β-cobalt hydroxide based on diffusion and reaction in organic gels. J Phys chem 112:7755–7757

Gamonchuang J, Poosimma P, Saito K, Khaorapapong N, Ogawa M (2016) The effect of alcohol type on the thickness of silica layer of Co_3O_4@SiO_2 core-shell particle. Colloids Surf A Physiochem Eng Asp 511:39–46

Hao YJ, Li FT, Zhao J, Liu RH, Wang XJ, Li YP, Liu Y (2016) Introduction of $CoCl_2{\cdot}6H_2O$ into Co_3O_4 for enhancement of hydroxyl radicals and effective charges separation. Dalton Trans 45(6):2444–2453

He T, Chen D, Jiao X (2004) Controlled synthesis of Co_3O_4 nanoparticles through oriented aggregation. Chem Mater 16:737–743

Hu Z, Xie Y, Wang Y, Xie L, Fu G, Jin X, Zhang Z, Yang Y, Wu H (2009) Synthesis of α-Cobalt Hydroxides with difference intercalated anions and effects of intercalated anions on their morphology, basal plane spacing, and capacitive property. J Phys Chem 113:12502–12508

Huang J, Ren H, Chen K, Shim J (2014) Controlled synthesis of porous Co_3O_4 micro/nanostructures and their photocatalysis property. Superlattices Microstruct 75:843–856

Jing X, Song S, Wang J, Ge L, Jamil S, Liu Q, Mann T, He Y, Zhang M, Wei H, Liu L (2012) Solvothermal synthesis of morphology controllable $CoCO_3$ and their conversion to CO_3O_4 for catalytic application. Powder Technol 217:624–628

Kim M, Huh Y (2011) Morphology-controlled synthesis of octahedron and hexagonal plate of Co_3O_4. Mater Lett 65:650–652

Li H, Fei GT, Fang M, Cui P, Guo X, Yan P, Zhang LD (2011) Synthesis of urchin-like Co_3O_4 hierarchical micro/nanostructures and their photocatalytic activity. Appl Surf Sci 257:6527–6530

Meng X, Feng M, Zhang H, Ma Z, Zhang C (2017) Solvothermal synthesis of cobalt/nickel layered double hydroxides for energy storage devices. J Alloy Compd 695:3522–3529

Mishra G, Dash B, Pandey S (2018) Layered double hydroxides: a brief review from fundamentals to application as evolving biomaterials. Appl Clay Sci 153:172–186

Neta P, Huie RE, Ross AB (1988) Rate constants for reactions of inorganic radicals in aqueous solution. J Phys Chem 17(3):1027–1284

Ni Y, Ge X, Zhang Z, Liu H, Zhu Z, Ye Q (2001) A simple reduction-oxidation route to prepare Co3O4 nanocrystals. Mater Res Bull 36:2383–2387

Petkova P, Nedkov V (2013) Behavior of Co^{2+} cations in the aqueous and alcoholic solution of $CoCl_2.6H_2O$. Acta Phys Pol A 123(2):207–208

Rahbani J, Ammar M, Al-Ghoul M (2013) Reaction-diffusion framework: the mechanism of the polymorphic transition of α- to β-Cobalt Hydroxide. J Phys Chem A 117:1685–1691

Rivas L, Gimeno O, Carbajo M, Borralho T (2009) Catalytic decomposition of potassium monopersulfate: influence of variables. World Acad Sci Eng Technol 57:218–222

Saputra E, Duan X, Pinem JA, Bahri S, Wang S (2017) Shape-controlled Co_3O_4 catalysts for advanced oxidation of phenolic contaminants in aqueous solutions. Sep Purif Technol 186:213–217

Saputra E, Muhammad S, Sun H, Ang H, Tadé MO, Wang S (2014) Shape-controlled activation of peroxymonosulfate by single crystal α-Mn_2O_3 for catalytic phenol degradation in aqueous solution. Appl Catal B 154–155:246–251

Shi P, Dai X, Zheng H, Li D, Yao W, Hu C (2014) Synergistic catalysis of Co_3O_4 and graphene oxide on Co3O4/GO catalysts for degradation of orange II in water by advanced oxidation technology based on sulfate radicals. Chem Eng J 240:264–270

Vinod CP (2010) Surface science as a tool for probing nanocatalysis phenomena. Catal Today 154:113–117

Warang T, Patel N, Fernandes R, Bazzanella N, Miotellop A (2013) Co_3O_4 nanoparticles assembled coatings synthesized by different techniques for photo- degradation of methylene blue dye. Appl Catal B 132–133:204–211

Yang H, Hu Y, Zhang X, Qui G (2004) Mechanochemical synthesis of cobalt oxide nanoparticles. Mater Lett 58:387–389

Yang Y, Huang K, Liu R, Wang L, Zeng W, Zhang P (2007) Shape-controlled synthesis of nanocubic Co3O4 by hydrothermal oxidation method. Trans Nonferrous Met Soc China 17:1082–1086

Yang Y, Jiang J, Lu X, Ma J, Liu Y (2015) Production of sulfate radical and hydroxyl radical by reaction of ozone with peroxymonosulfate: A novel advanced oxidation process. Environ Sci Technol 49:7330–7339